ELECTROWEAK-BOSON PRODUCTION FROM SMALL-TO-LARGE COLLISION SYSTEMS WITH ALICE AT THE LHC*

Shingo Sakai

for the ALICE Collaboration

University of Tsukuba, Japan

Received 10 August 2022, accepted 26 September 2022, published online 14 December 2022

Electroweak bosons, $W^{\pm}$ and Z^0, are massive weakly-interacting particles insensitive to the strong interaction. Therefore, they are unique probes in *pp* and heavy-ion collisions, and provide a medium-blind probe of the initial state of the heavy-ion collision. In the ALICE experiment, the production of $W^{\pm}$ and Z^0 is studied by exploiting their semileptonic decay channels in a wide rapidity region. In this contribution, the results in *pp* collisions at $\sqrt{s} = 13$ TeV, *p*–Pb collisions at $\sqrt{s_{NN}} = 8.16$ TeV, and Pb–Pb collisions at $\sqrt{s_{NN}} = 5.02$ TeV are reported.

DOI:10.5506/APhysPolBSupp.16.1-A127

1. Introduction

The $W^{\pm}$ and Z^0 bosons have large masses, and they are predominantly produced via quark–antiquark annihilation [1] in an early stage of *pp* and heavy-ion collisions. In *pp* collisions, their production has been successfully described by calculations based on perturbative QCD (pQCD). In addition, the production of W^+ and W^- is sensitive to the light-quark parton distribution function [2]. In recent measurements of particle production in high-multiplicity events in *pp* collisions at $\sqrt{s} = 13$ TeV, a faster than linear increasing trend of the self-normalised yields with multiplicity is observed [3]. The comparison with models suggests that accounting for multiple parton interactions (MPI) and color-reconnection (CR) effects is important to describe the trends observed in data [4]. Since $W^{\pm}$ and Z^0 bosons are colorless, their production is expected to be less sensitive to CR effects than the hadron one. Therefore, their measurements give insight into MPI in high-multiplicity events and role of CR. In heavy-ion collisions, $W^{\pm}$ and Z^0

* Presented at the 29th International Conference on Ultrarelativistic Nucleus–Nucleus Collisions: Quark Matter 2022, Kraków, Poland, 4–10 April, 2022.

bosons are expected to carry the information of the initial-state nuclear effects, such as the modification of the parton distribution functions of the nucleus (nPDFs), because they do not interact with the medium constituents.

2. ALICE apparatus and $W^{\pm}$ and Z^0 bosons reconstruction

The analysis was performed using data recorded in pp collisions at $\sqrt{s} =$ 13 TeV, p–Pb collisions at $\sqrt{s_{NN}}$ = 8.16 TeV, and Pb–Pb collisions at $\sqrt{s_{NN}}$ = 5.02 TeV with the ALICE detector. The details of the detector and its performance are described in Ref. [5].

At midrapidity, the $W^{\pm}$ boson candidates are reconstructed by measuring the electrons from their semileptonic decays with the Time Projection Chamber (TPC) and the Electromagnetic Calorimeter (EMCal). In this analysis, electrons with $p_{\rm T}$ larger than 30 GeV/c are used for which $W^{\pm}$-boson decay contribution is dominant. The electrons are identified based on their energy loss (dE/dx) in the TPC, and on the energy-to-momentum ratio ($E/p \sim 1$), where the energy is measured in the EMCal. In addition, an isolation criterion on the energy information around the electron candidates is applied to remove the background, which is mainly composed of heavy-flavour-hadron decay electrons. The additional contribution from Z^0-boson decays, estimated using the POWHEG simulation [6], is statistically subtracted.

At forward rapidity, the $W^{\pm}$-boson candidates are reconstructed in the single-muon channel with the muon spectrometer. The signal (muons from $W^{\pm}$-boson decay) and background (muons from Z^0-boson and heavy-flavour-hadrons decays) is separated by fitting the measured single-muon transverse momentum spectrum ($p_{\rm T}^{\mu} > 10$ GeV/c) with the templates extracted using Monte Carlo simulations. The simulations for muons from $W^{\pm}$- and Z^0-boson decays were performed with the event generator POWHEG [6], and for heavy-flavour hadrons were based on FONLL QCD calculation [7, 8]. In the POWHEG simulation for p–Pb and Pb–Pb collisions, the lead nucleus isospin was taken into account by weighting the proton and neutron contributions.

The Z^0 bosons are reconstructed with an invariant mass analysis in the dimuon decay channel $Z^0 \rightarrow \mu^+\mu^-$ with $p_{\rm T}^{\mu} > 20$ GeV/c in the rapidity range of $2.5 < y < 4$.

3. Results

3.1. $W^{\pm}$ production in pp collisions at $\sqrt{s} =$ 13 TeV

Figure 1 shows the $p_{\rm T}$ differential cross sections for electrons from W^- (left) and positrons from W^+ (right) in $|y| < 0.6$ in pp collisions at $\sqrt{s} =$ 13 TeV. The measured cross sections are compared with the POWHEG simulations [6] which are based on NLO pQCD. The CT10NLO PDFs [9] were used in these calculations, and the bands represent the theoretical uncertainty from the PDFs. The measured cross sections are consistent with the POWHEG calculations within experimental and theoretical uncertainties.

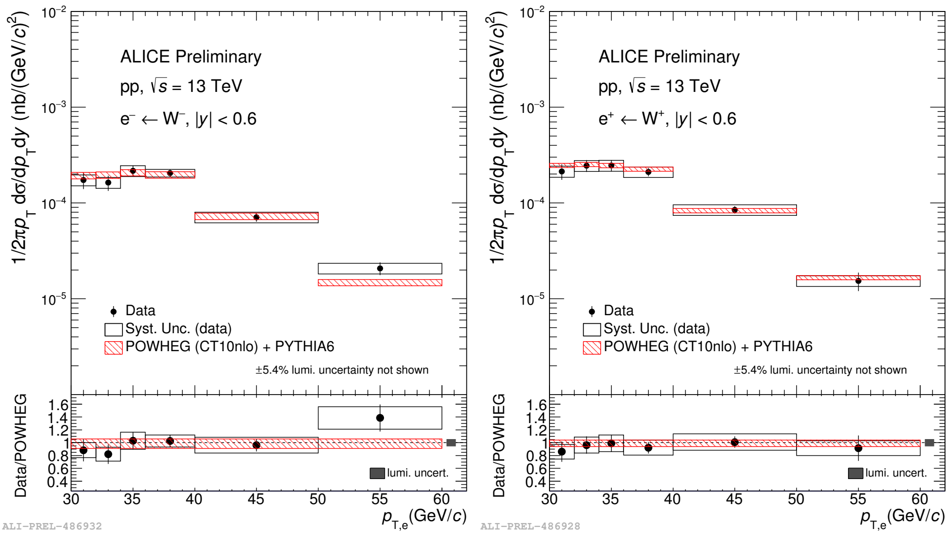

Fig. 1. (Color online) Cross section of electrons (left) and positrons (right) from W^- and W^+decay in pp collisions at $\sqrt{s} = 13$ TeV, respectively, compared with the POWHEG calculations with CT10NLO PDFs (red/gray striped bands).

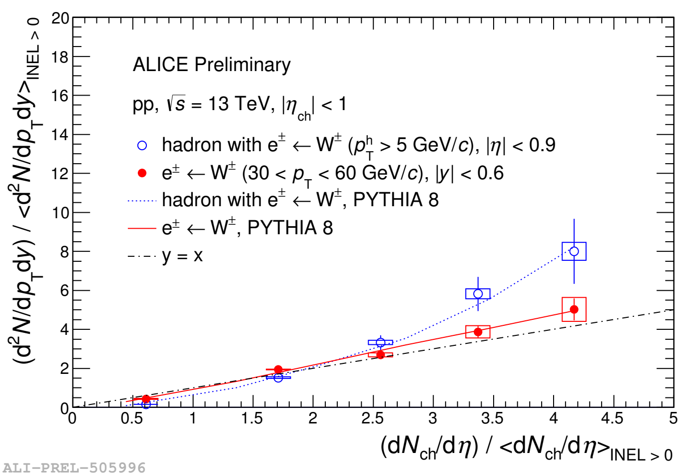

Fig. 2. Self-normalised yields of $e^{\pm} \leftarrow W^{\pm}$ and the associated hadrons *vs.* normalised charged-particle pseudorapidity density compared with the expectation from the PYTHIA 8 [10] simulation including CR effects [11].

Figure 2 shows the self-normalised yields of electrons from $W^{\pm}$ boson and charged hadrons in association with W boson as a function of normalised charged-particle multiplicity at midrapidity in pp collisions at $\sqrt{s} = 13$ TeV. The production of electrons from $W^{\pm}$ bosons is linear with respect to the multiplicity. On the other hand, the trend of the associated hadron production is faster than linear. The result is compared with the PYTHIA 8 predictions [10] including MPI and CR. The predictions are consistent with the data.

3.2. $W^{\pm}$ production in p–Pb collisions at $\sqrt{s_{NN}} = 8.16$ TeV and Pb–Pb collisions at $\sqrt{s_{NN}} = 5.02$ TeV

Figure 3 shows the lepton-charge asymmetry at forward and backward rapidity for muons from $W^{\pm}$-boson decays [12]. The result shows the clear lepton-charge asymmetry at forward and backward rapidity regions. The model calculations based on pQCD (MCFM [13]) with and without the nuclear modification of the parton distribution functions (EPPS16 [14] and nNNPDF2.0 [15]) reproduce the measured asymmetry at both forward and backward rapidity. However, the significant deviation between data and models is observed at large rapidity.

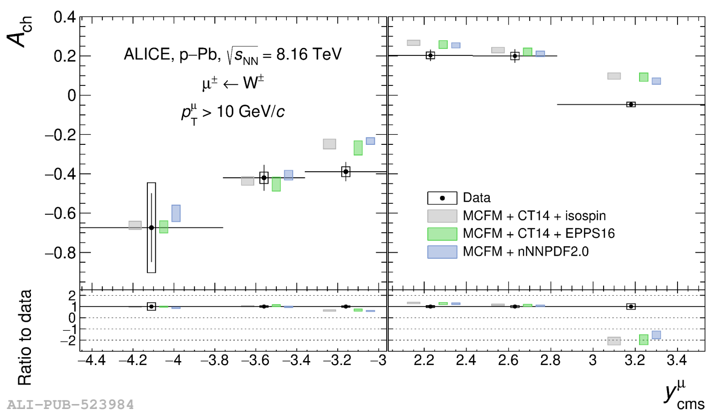

Fig. 3. Lepton-charge asymmetry as a function of rapidity for muons from $W^{\pm}$-boson decays in p–Pb collisions at $\sqrt{s_{NN}} = 8.16$ TeV. The result is compared with theoretical calculations with and without nuclear effects.

The $W^{\pm}$-boson production yield in Pb–Pb collisions at $\sqrt{s_{NN}} = 5.02$ normalised by the nuclear overlap function ($\langle T_{AA} \rangle$), as a function of the centrality, is shown in Fig. 4. The result is compared with the HG-PYTHIA [16] calculations scaled with the measured value in 0–90% centrality. Data and model predictions are consistent within uncertainties.

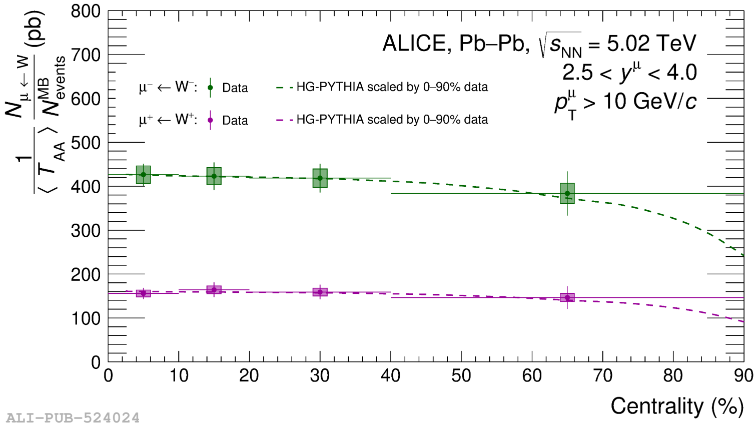

Fig. 4. Normalised invariant yield of muons from W^+ and W^- as a function of the centrality in Pb–Pb collisions at $\sqrt{s_{NN}} = 5.02$ TeV. The measured production is compared with the HG-PYTHIA calculations [16].

3.3. Z production in Pb–Pb collisions at $\sqrt{s_{NN}} = 5.02$ TeV

Production cross section of $\mu^+\mu^-$ from Z^0-boson decays in Pb–Pb collisions at $\sqrt{s_{NN}} = 5.02$ is shown in Fig. 5. The result is normalised by the nuclear overlap function. The result is also compared with the theoretical calculations based on MCFM and FEWZ with and without nuclear PDF (EPPS16, nCTEQ15, and EPS09s [17]). The calculations with nuclear PDF are in good agreement with the data. On the other hand, the calculation without the modification (MCFM + CT14) is 3.4σ higher than the data.

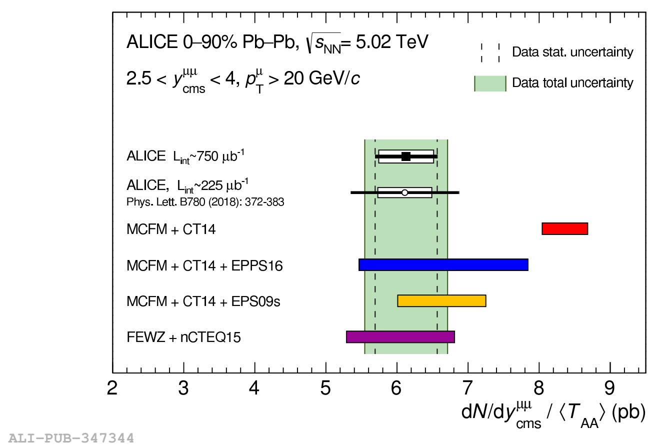

Fig. 5. Production cross section of $\mu^+\mu^-$ from Z^0-boson decays in Pb–Pb collisions at $\sqrt{s_{NN}} = 5.02$ TeV. The result is also compared to model calculations with and without nuclear PDF (EPPS16, nCTEQ15, and EPS09s).

4. Summary

The production of $W^{\pm}$ and Z^0 bosons was measured with the ALICE experiment in pp collisions at $\sqrt{s} = 13$ TeV, p–Pb collisions at $\sqrt{s_{NN}} = 8.16$ TeV, and Pb–Pb collisions at $\sqrt{s_{NN}} = 5.02$ TeV. In the pp collisions, the measured cross sections for $e^{\pm} \leftarrow W^{\pm}$ are in good agreement with theoretical predictions based on pQCD. The production shows an increasing linear trend as a function of charged-particle multiplicity. In the p–Pb collisions, the lepton-charge asymmetry at forward and backward rapidity for muons from $W^{\pm}$-boson decays was measured. The measurements were compared with models with and without nuclear modification of the PDFs, and significant deviations between data and models are found at large rapidity in the forward region. In Pb–Pb collisions, $\mu^{\pm} \leftarrow W^{\pm}$ and $Z^0 \rightarrow \mu^+\mu^-$ were measured at forward rapidity. The normalised invariant yield of muons from W^+ and W^- as a function of the centrality is consistent with the HG-PYTHIA [16] calculations. The Z^0-boson production cross section is in good agreement with the model including the nuclear effects, whereas a model without these effects is 3.4σ higher than the data.

REFERENCES

[1] M. Schott, M. Dunford, *Eur. Phys. J. C* **74**, 2916 (2014).
[2] H. Paukkunen, C.A. Salgado, *J. High Energy Phys.* **1103**, 071 (2011).
[3] ALICE Collaboration (S. Acharya *et al.*), *Phys. Lett. B* **810**, 135758 (2020).
[4] ALICE Collaboration (S. Acharya *et al.*), *Phys. Lett. B* **829**, 137065 (2022).
[5] ALICE Collaboration (K. Aamodt *et al.*), *J. Instrum.* **3**, S08002 (2008).
[6] S. Alioli, P. Nason, C. Oleari, E. Re, *J. High Energy Phys.* **2008**, 060 (2008).
[7] M. Cacciari, M. Greco, P. Nason, *J. High Energy Phys.* **1998**, 007 (1998).
[8] M. Cacciari, S. Frixione, P. Nason, *J. High Energy Phys.* **2001**, 006 (2001).
[9] H.L. Lai *et al.*, *Phys. Rev. D* **82**, 074024 (2010).
[10] T. Sjöstrand *et al.*, *Comput. Phys. Commun.* **191**, 159 (2015).
[11] J.R. Christiansen, P.Z. Skands, *J. High Energy Phys.* **1508**, 003 (2015).
[12] ALICE Collaboration, `arXiv:2204.10640 [nucl-ex]`.
[13] R. Boughezal *et al.*, *Eur. Phys. J. C* **77**, 7 (2017).
[14] K.J. Eskola, P. Paakkinen, H. Paukkunen, C.A. Salgado, *Eur. Phys. J. C* **77**, 163 (2017).
[15] R. Abdul Khalek, J.J. Ethier, J. Rojo, G. van Weelden, *J. High Energy Phys.* **2020**, 183 (2020).
[16] C. Loizides, A. Morsch, *Phys. Lett. B* **773**, 408 (2017).
[17] I. Helenius, K.J. Eskola, H. Honkanen, C.A. Salgado, *J. High Energy Phys.* **1207**, 073 (2012).